Infrared transmission study of crystal-field excitations in $La_{2-x-y}Nd_xSr_yCuO_4$

G. Riou,* S. Jandl, and M. Poirier
Centre de Recherche sur les Propriétés Électroniques des Matériaux Avancés, Département de Physique, Université de Sherbrooke, Sherbrooke, Canada J1K 2R1

V. Nekvasil, M. Maryško, J. Fábry, and K. Jurek
Institute of Physics, Czech Academy of Sciences, Cukrovarnická 10, 162 53 Praha 6, Czech Republic

M. Diviš
Department of Electron Systems, Charles University, Ke Karlovu 2, 121 16 Praha 2, Czech Republic

J. Hölsä
Department of Chemistry, University of Turku, FIN-20014 Turku, Finland

I. M. Sutjahja† and A. A. Menovsky
Van der Waals-Zeeman Instituut, Universiteit van Amsterdam, Valckenierstraat 65, 1018 XE, Amsterdam, The Netherlands

S. N. Barilo, S. V. Shiryaev, and L. N. Kurnevich
Institute of Solid State and Semiconductors Physics, National Academy of Science, 17 P. Brovka street, Minsk 220072, Belarus

(Received 6 June 2002; revised manuscript received 29 August 2002; published 16 December 2002)

We report an infrared crystal field study of $La_{2-x-y}Nd_xSr_yCuO_4$ single crystals for ($x=0.35$, $y=0$), ($x=0.34$, $y=0.14$), and ($x=0.42$, $y=0.19$). Nd^{3+} crystal field excitations from the ground state multiplet $^4I_{9/2}$ to the $^4I_{11/2}$, $^4I_{13/2}$, $^4I_{15/2}$, and $^4F_{3/2}$ excited multiplets are observed. A precise set of crystal field parameters, that reproduces the Nd^{3+} electronic levels in all the samples as well as the $La_{1.65}Nd_{0.35}CuO_4$ susceptibility measurements as a function of temperature, is determined. A very strong Ising-like anisotropy of the low-temperature Nd^{3+} magnetic moment is related to a large value of the second rank crystal field parameter B_{20}. In addition to the Nd^{3+} C_{4v} symmetry regular site a second one, of lower symmetry, is detected and related to possible stripe formation.

DOI: 10.1103/PhysRevB.66.224508 PACS number(s): 74.72.Dn, 71.70.Ch, 71.70.Gm, 75.10.Dg

I. INTRODUCTION

Ordered charges and spin domains (stripes and phase separations) in layered cuprates[1] and other oxides[2,3] could play a key role in the mechanism of high temperature superconductivity (HTSC).[4] Probing locally these charge and spin inhomogeneities has recently become an important issue.[5,6]

Rare-earth (RE) crystal field (CF) excitations, to which the electronic and magnetic properties are very sensitive, have been successfully used to study various physical properties of the HTSC and their parent compounds.[7] Particularly, Raman scattering and infrared transmission spectroscopies have proven to be valuable techniques in the determination of the rare-earth CF excitations in both electron[8–11] and hole doped cuprates.[12,13] Since the rare-earth ions are located in the vicinity of the copper-oxygen planes, the presence of doped charge carriers in inhomogeneous structures such as stripes or clusters affects their CF energy levels.

The study of CF excitations in $La_{2-x-y}Nd_xSr_yCuO_4$ compounds, which are known to exhibit phase separation and stripe formation,[1] would help to characterize the effect of charge redistribution on the Nd^{3+} CF levels. Many phase transitions are observed in these materials involving rotations of the CuO_6 octahedra.[14–16] The high-temperature tetragonal (HTT) ($I4/mmm$), the low-temperature orthorhombic (LTO) ($Bmab$) and the low-temperature tetragonal (LTT) ($P4_2/ncm$) phases have been characterized by Raman spectroscopy[17] and neutron scattering,[18,19] while Lampakis *et al.*[20] have observed two broad Raman excitations around 150 and 380 cm^{-1} in $La_{2-x}Sr_xCuO_4$ compatible with stripe formation.

In this article, we study the Nd^{3+} CF excitations in $La_{2-x-y}Nd_xSr_yCuO_4$. The principal objectives are (i) to report the Nd^{3+} CF excitations in single crystals as detected by infrared transmission spectroscopy, (ii) to determine the CF parameters that describe the CF interaction and fit the measured magnetic susceptibility, (iii) to discuss the origin of the additional Nd^{3+} CF excitations.

II. EXPERIMENTS

Infrared transmission spectra of $La_{2-x-y}Nd_xSr_yCuO_4$ ($x=0.35$, $y=0$) sample 1 as grown and reduced at 800 °C in Ar atmosphere, ($x=0.34$, $y=0.14$) sample 2, and ($x=0.42$, $y=0.19$) sample 3 single crystals have been recorded as a function of temperature. Samples 1 and 3 were grown by the travelling solvent floating zone technique (image furnace)[21] while sample 2 was obtained by the flux method.[22] Considering their various phase transitions, samples 1 and 3 have been further characterized by specific heat measurements, carried out using the relaxation method

by means of a commercial Quantum Design PPMS magnetometer, and by Raman spectroscopy: sample 1 is in the LTO phase at room temperature and undergoes a LTO→LTT phase transition at 80 K, while sample 3 is in the HTT phase at room temperature and in the LTO phase below 275 K. Sample 2 is according to the phase diagram of Ref. 23 in the LTT phase below 60 K. A preliminary Raman study has enabled us to orient the samples and to characterize their inhomogeneities. For the infrared study, the samples were mounted on a helium closed cycle cryostat cold finger and 0.5 cm^{-1} resolution transmission spectra were obtained in the 1800–15 000 cm^{-1} energy range with a Fourier transform interferometer (BOMEM DA3.002) equipped with InSb and Si detectors, quartz-halogen and globar sources as well as CaF_2 and quartz beamsplitters. The composition homogeneity of sample 1 was measured using an electron microprobe x-ray analyzer JXA 733 (JEOL) equipped with WD spectrometers. Experimental data were processed by the XPP correction program (SAMX). The oxygen concentration was estimated from stoichiometry.

In order to further characterize samples 1 and 3, microwave conductivity at 16.5 GHz was measured, in the 4.2–300 K temperature range, using the standard cavity perturbation contactless technique which is well suited for the measurements of electrical conductivity in anisotropic materials.[24,25] The microwave conductivity measurements at 16.5 GHz show that sample 3 displays a superconducting transition around 20 K and the low *c*-axis plasma frequency ~ 150 cm^{-1} (Ref. 26) renders its infrared transmission possible. Sample 1 magnetization and magnetic susceptibility parallel and perpendicular to the CuO_2 planes were measured using a superconducting quantum interference device magnetometer Quantum Design MPM-5S in the temperature range from 4.5 to 300 K.

III. RESULTS AND DISCUSSION

Sample 1, which is in the LTO phase at room temperature, undergoes a gradual LTO→LTT phase transition around 80 K.[14] The temperature evolution of the sample 1 five Raman active phonons, in the $x(zz)\bar{x}$ configuration, confirms its orientation [Fig. 1(a)]; hardening of the 120 cm^{-1} phonon between 300 and 100 K [inset of Fig. 1(a)] is followed by a softening at lower temperature indicating the occurrence of the LTO→LTT transition.[17] This phase transition appears in the specific heat measurements around 80 K (Fig. 2). Raman active excitations that are not predicted by group theory are observed around 150 and 380 cm^{-1} [Fig. 1(b)]. The C_{4v} symmetry crystal field at the Nd^{3+} site lifts the $(2J+1)$-fold degeneracy of the $4f^3$ state *J* multiplets. Assuming a perfect orientation of the crystal and the absence of depolarization effects as well as of disorder, $\Gamma_6 \rightarrow \Gamma_6$ and $\Gamma_7 \rightarrow \Gamma_7$ transitions are observed for $\mathbf{E} \| \mathbf{z}$ while $\Gamma_6 \rightarrow \Gamma_7$ transitions are observed for $\mathbf{E} \perp \mathbf{z}$.

Similarly to as grown cerium doped Nd_2CuO_4 and Pr_2CuO_4,[8,10] more infrared absorption bands than expected from the Nd^{3+} regular sites, are observed. They are due to nonregular Nd^{3+} sites which frequencies are influenced by reduction, Sr doping, local charge fluctuations, and/or distor-

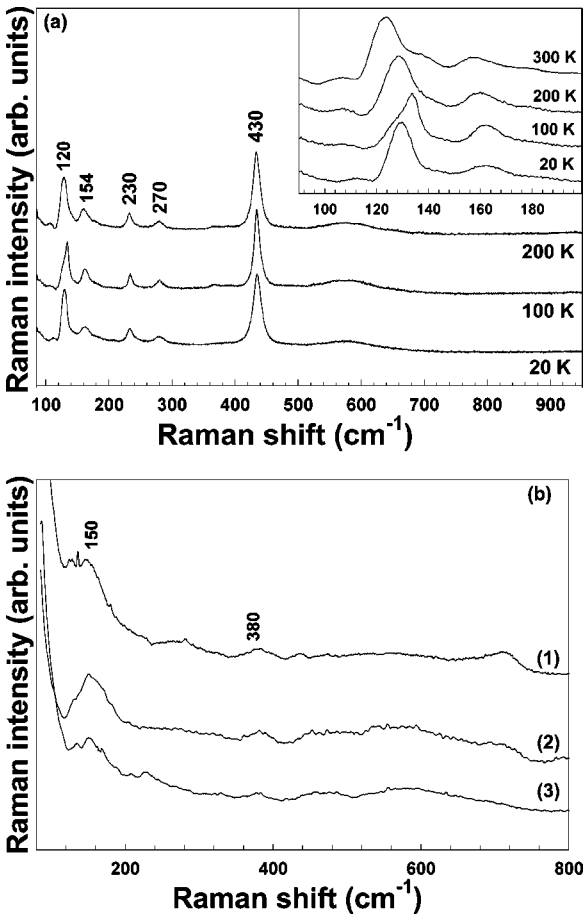

FIG. 1. (a) Temperature evolution of the Raman-active phonons of $La_{1.65}Nd_{0.35}CuO_4$ in the $x(zz)\bar{x}$ configuration. Inset: A zoom around 120 cm^{-1}. (b) $La_{1.65}Nd_{0.35}CuO_4$ (1), $La_{1.52}Nd_{0.34}Sr_{0.14}CuO_4$ (2), and $La_{1.49}Nd_{0.42}Sr_{0.19}CuO_4$ (3) Raman-active phonons in the $y(xx)\bar{y}$ configuration at 78 K.

sions. CF absorption bands are shown in Figs. 3,4,5. In order to determine the parameters that describe the CF interactions at the regular sites, the less affected absorption bands by doping are considered.

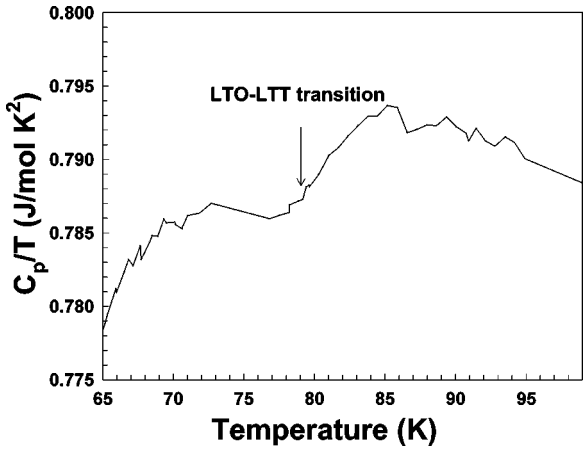

FIG. 2. $La_{1.65}Nd_{0.35}CuO_4$ specific heat measurement as a function of temperature from 65 to 100 K.

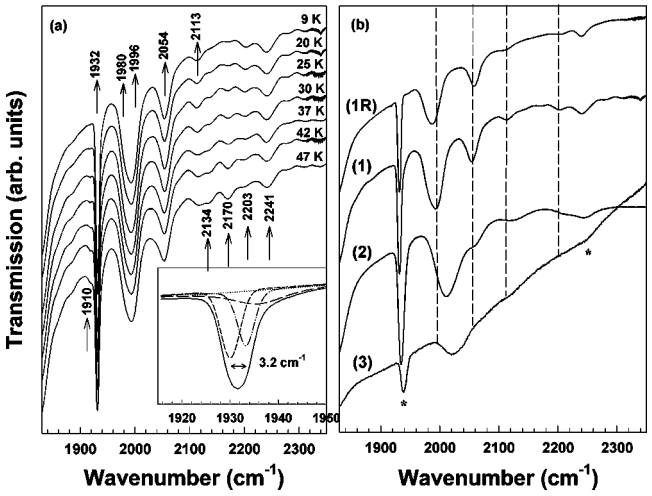

FIG. 3. (a) Temperature evolution of the $^4I_{9/2}\rightarrow{}^4I_{11/2}$ transitions in $La_{1.65}Nd_{0.35}CuO_4$ for $\mathbf{E}\|\mathbf{z}$. Inset: Fitting of the 1932 cm^{-1} absorption band at 9 K. (b) Low-temperature spectra at 9 K of the as grown (1) and reduced (1R) $La_{1.65}Nd_{0.35}CuO_4$, $La_{1.52}Nd_{0.34}Sr_{0.14}CuO_4$ (2) and $La_{1.49}Nd_{0.42}Sr_{0.19}CuO_4$ (3). Asterisks indicate absorptions associated with the regular Nd^{3+} sites.

The temperature evolution of the $^4I_{9/2}\rightarrow{}^4I_{11/2}$ transitions is presented in Fig. 3(a). The absorption bands at (1932 cm^{-1}) and (1980, 2241 cm^{-1}) are associated with ($\Gamma_6\rightarrow\Gamma_7$) and ($\Gamma_6\rightarrow\Gamma_6$) transitions, respectively. The bands at 1910 and 2170 cm^{-1} correspond to transitions from the thermally populated 70 cm^{-1} Γ_7 level to Γ_6 levels. The selection rules are not rigorously respected due to depolarization effects. The presence of strontium induces a broadening and a shift of the absorption bands indicated by dashed lines in Fig. 3(b). The additional bands, detected at 1996, 2054, 2113 and 2203 cm^{-1}, are associated with nonregular Nd^{3+} sites.

The temperature evolution of the $^4I_{9/2}\rightarrow{}^4I_{13/2}$ transitions is presented in Fig. 4(a). The absorption bands at (3883,

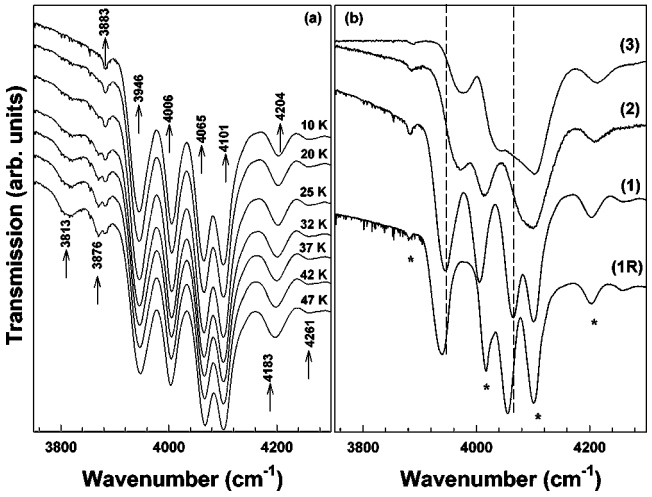

FIG. 4. (a) Temperature evolution of the $^4I_{9/2}\rightarrow{}^4I_{13/2}$ transitions in $La_{1.65}Nd_{0.35}CuO_4$ for $\mathbf{E}\|\mathbf{z}$. (b) Low-temperature spectra at 9 K of the as grown (1) and reduced (1R) $La_{1.65}Nd_{0.35}CuO_4$, $La_{1.52}Nd_{0.34}Sr_{0.14}CuO_4$ (2), and $La_{1.49}Nd_{0.42}Sr_{0.19}CuO_4$ (3). Asterisks indicate absorptions associated with the regular Nd^{3+} sites.

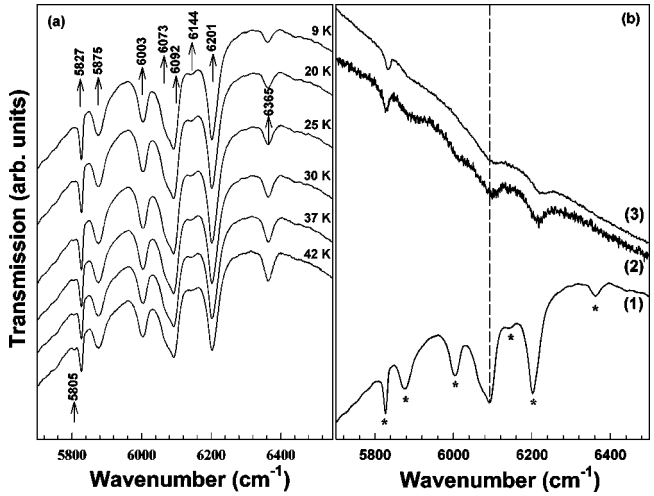

FIG. 5. (a) Temperature evolution of the $^4I_{9/2}\rightarrow{}^4I_{15/2}$ transitions in $La_{1.65}Nd_{0.35}CuO_4$ for $\mathbf{E}\|\mathbf{z}$. (b) Low-temperature spectra at 9 K of $La_{1.65}Nd_{0.35}CuO_4$ (1), $La_{1.52}Nd_{0.34}Sr_{0.14}CuO_4$ (2), and $La_{1.49}Nd_{0.42}Sr_{0.19}CuO_4$ (3). Asterisks indicate absorptions associated with the regular Nd^{3+} sites.

4101, 4204 cm^{-1}) and (4006 cm^{-1}) are associated with ($\Gamma_6\rightarrow\Gamma_7$) and ($\Gamma_6\rightarrow\Gamma_6$) transitions, respectively. The band at 3813 cm^{-1} corresponds to a transition from the thermally populated 70 cm^{-1} Γ_7 level to a Γ_7 level while the absorption at 3876 cm^{-1} is associated with a transition from the 130 cm^{-1} Γ_6 level to a Γ_7 level. Broadenings and small shifts of the absorption bands are observed with the increase of the strontium content [Fig. 4(b)]. The additional absorptions at 3946, 4065, and 4261 cm^{-1} are associated with the nonregular Nd^{3+} sites.

Finally, the temperature evolution of the $^4I_{9/2}\rightarrow{}^4I_{15/2}$ transition is presented in Fig. 5(a). The absorption bands at (5827, 6003, 6144, 6365 cm^{-1}) and (5875, 6201 cm^{-1}) are associated with ($\Gamma_6\rightarrow\Gamma_6$) and ($\Gamma_6\rightarrow\Gamma_7$) transitions, respectively. The band at 5805 cm^{-1} corresponds to a transition from the thermally populated 70 cm^{-1} Γ_7 level to a Γ_7 level. Broadenings and small shifts of the absorption bands are also observed with the increase of strontium content [Fig. 5(b)]. Additional absorptions at 6073 and 6092 cm^{-1} are associated with the nonregular Nd^{3+} sites.

In the following, we analyze the optical data using the CF Hamiltonian written as

$$H_{\mathrm{CF}}=\sum_{k,q} B_{kq}C_q^k, \tag{1}$$

where C_q^k is the qth component of a spherical tensor operator of rank k, and B_{kq} the corresponding CF parameter. In the C_{4v} symmetry Nd^{3+} sites only five CF parameters B_{20}, B_{40}, B_{44}, B_{60}, and B_{64}, are nonzero. These parameters are determined by solving numerically the inverse secular problem where the CF levels deduced from the optical spectra are taken to be the eigenvalues of the secular equation of H_{CF}. However, as mentioned previously, the large number of observed bands indicates the presence of at least one additional Nd^{3+} site. Moreover, to our knowledge, no data, which

TABLE I. Nd^{3+} ion CF parameters (in cm^{-1}) in $La_{1.65}Nd_{0.35}CuO_4$. Given in brackets are the mean errors associated with the fitting parameters.

B_{kq}	Theory	Fit
B_{20}	1123	1518 (5)
B_{40}	675	−863 (6)
B_{44}	−238	−200 (6)
B_{60}	381	372 (4)
B_{64}	866	914 (3)

could serve as an initial estimate for the parameters B_{kq} in the studied compounds, are available. Therefore, our CF analysis was made in several steps.

In the first step, in analogy with Ce-doped Nd_2CuO_4,[10] we ascribed the experimental CF levels, which do not depend on the Sr doping, to the regular Nd^{3+} site. The corresponding levels at 0, 70, 130, 1932, 2241, 4101, 5827, 5875, 6003, 6201, and 6365 cm^{-1} were fitted by the least-squares method in which the calculations using a semiphenomenological superposition model (SM) and an *ab initio* method based on the density functional theory (for details see Ref. 13) provided an initial estimate for the CF parameters. The structure parameters available for the ideal tetragonal $I4/mmm$ (HTT) crystallographic structure of La_2CuO_4 (so-called T structure)[27] have been considered in these calculations. In the following steps we have also included, among the input data, the levels that match the calculated ones (1980, 3883, 4006, 4204, and 6144 cm^{-1}) and obtained the CF parameters given in Table I.

The resulting best-fit values are compared with the theoretical ones in Table I, the free-ion energies of the ^4I_J multiplets, varied along the CF parameters in fitting the data, are 0 ($J=9/2$), 1872 ($J=11/2$), 3833 ($J=13/2$), and 5880 ($J=15/2$) cm^{-1}. It is to be noted that both sets of the CF parameters in Table I are rather similar except for the B_{40} parameter sign.

Our SM calculations indicate that the B_{40} parameter sign changes at the transition from the undistorted HTT structure to the low-temperature distorted structures. In the LTO and LTT phases, this tendency is associated with the tilting of the apical oxygen from the z axis as well as with the displacement of the two next nearest oxygen ligands closer to the Nd^{3+} ion (see, e.g., Refs. 14,28). The remaining CF parameters are not influenced significantly by this distortion.

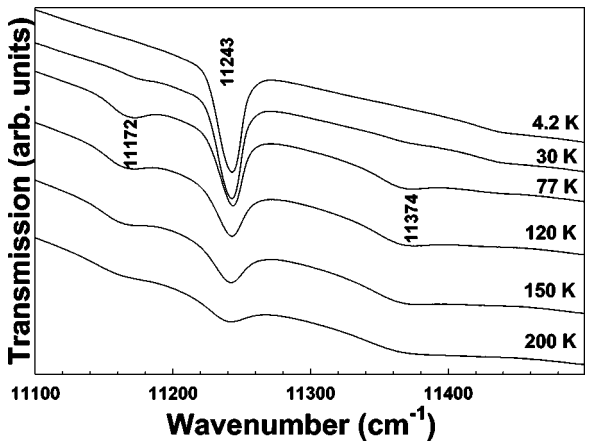

FIG. 6. Temperature evolution of the $^4I_{9/2} \rightarrow {}^4F_{3/2}$ transitions in $La_{1.65}Nd_{0.35}CuO_4$ for $\mathbf{E}\|\mathbf{z}$.

The CF levels, calculated using the best-fit set of the B_{kq} parameters, are compared with the experimental ones in Table II confirming that the crystal field at the regular Nd^{3+} sites can be well described by the C_{4v} symmetry Hamiltonian. We note that we have detected several transitions in the 10 000 to 15 000 cm^{-1} energy range. These lines are particularly difficult to assign mainly due to the scarcity of the data and the overlap of the J multiplets. The only exceptions are the levels at 11 243 and 11 444 (11 374+70 =11 444) cm^{-1} ascribed to the CF splitting of the $^4F_{3/2}$ multiplet (Fig. 6). The observed splitting (201 cm^{-1}) of the $^4F_{3/2}$ multiplet compares favorably with the theoretical value of 181 cm^{-1} as obtained by diagonalization of the free-ion Hamiltonian[29] together with the CF Hamiltonian [Eq. (1)], using the best-fit parameters of Table I. This agreement provides an independent test of the reliability of these parameters, B_{20} in particular.

The inelastic neutron scattering study, performed by Rœpke *et al.* in $La_{2-x-y}Nd_xSr_yCuO_4$ for $y \neq 0$,[30] shows that the observed quasielastic Lorentzian line above 80 K transforms into a mixed quasielastic Lorentzian-Gaussian line below 80 K, which is considered as a direct indication for

TABLE II. Energies (in cm^{-1}) and symmetries of Nd^{3+} ^4I term levels in $La_{1.65}Nd_{0.35}CuO_4$ associated with the regular and the nonregular sites, respectively (± 1 cm^{-1}).

$^4I_{9/2}$			$^4I_{11/2}$			$^4I_{13/2}$				$^4I_{15/2}$			
Fit		regular	Fit		regular	nonregular	Fit		regular	nonregular	Fit		regular	nonregular
Γ_6	-2	0	Γ_7	1940	1932		Γ_7	3882	3883		Γ_6	5824	5827	
Γ_7	70	70	Γ_6	1972	1980 (± 5 cm^{-1})	1996	Γ_7	3919			Γ_7	5876	5875	
Γ_6	132	130	Γ_6	2035		2054	Γ_6	3961		3946	Γ_7	5965		
Γ_7	309		Γ_7	2091		2113	Γ_6	4007	4006		Γ_6	6005	6003	6073
Γ_6	444		Γ_7	2188		2203	Γ_7	4098	4101	4065	Γ_6	6146	6144	6092
			Γ_6	2240	2241		Γ_7	4208	4204		Γ_7	6200	6201	
							Γ_6	4217		4261	Γ_6	6368	6365	
											Γ_7	6429		

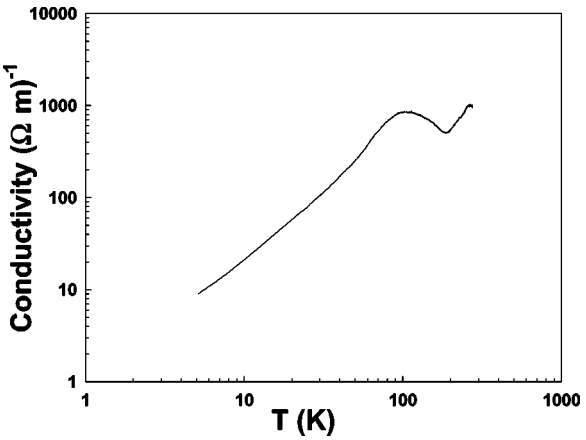

FIG. 7. *xy* plane $La_{1.65}Nd_{0.35}CuO_4$ microwave conductivity at 16.5 GHz as a function of temperature on a log-log scale.

spatial inhomogeneities in the CuO_2 planes. The detection of Raman active excitations at 150 and 380 cm^{-1} [Fig. 1(b)] confirms the expected phase separation in the studied samples,[20] which translates in Nd^{3+} nonregular sites. We tentatively associate the regular sites with hole-free antiferromagnetic regions and the nonregular sites with hole-rich regions in the samples. The atomic scale charge inhomogeneities, forming stripes in some cuprates, provoke local structural deformations (see, e.g., Refs. 17,31–33). The extra charge and the local deformations in the vicinity of the nonregular R^{3+} sites were considered in several point-charge model CF calculations.[6,34,35] Sufficiently detailed structural data based on the atomic pair distribution function (PDF) are available only for $Nd_{2-x}Ce_xCuO_4$.[33] Using this data, a SM-based modeling of the CF interaction at the nonregular Nd^{3+} sites has shown that the charge-transfer induced structural deformation, rather than the transferred charge itself, provokes the observed $\leqslant 50$ cm^{-1} shifts of the Nd^{3+} CF levels with respect to the regular sites.[10,36] Similarly to the $Nd_{2-x}Ce_xCuO_4$ study, the observed $\leqslant 40$ cm^{-1} Sr-doping induced shifts of CF transitions (Figs. 3,4,5, Table II) are ascribed partially to local structural deformations. While PDF,[32] EXAFS,[37] and Raman[17] studies of $La_{2-x-y}Nd_xSr_yCuO_4$ indicate such a deformation, they do not provide the crucial precise information, about the relative positions of oxygen ions with respect to the Nd^{3+} ions, for the theoretical modeling. Moreover, the dependance of these nonregular sites CF excitations on reduction and Sr doping proves that they are also sensitive to charge density since their shift to higher energies increases with hole doping. Sample 1, if stoichiometric, is expected to exhibit an insulating behavior as in Pr_2CuO_4 (Ref. 8) and Nd_2CuO_4.[25] However, the sample 1 *xy* plane conductivity is quite high at low temperature as shown in Fig. 7. As observed in other compounds, the microwave conductivity decreases with temperature in a semiconducting fashion, and the structure appearing around 150 K, whose origin is still unknown, appears also in Nd_2CuO_4 microwave conductivity data.[25] Despite the fact that the temperature profile is very similar to what is found in other compounds, the high microwave conductivity is consistent with the presence of some impurity band. This implies

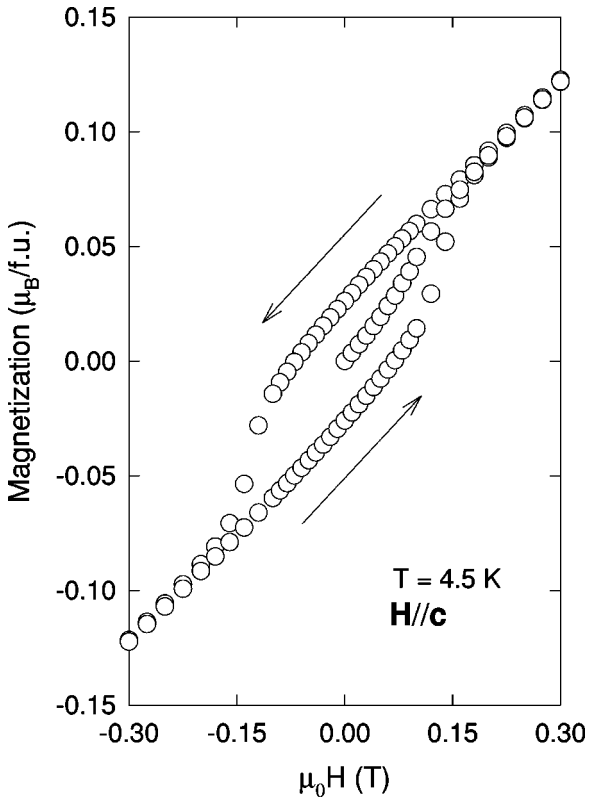

FIG. 8. Magnetic hysteresis curve for $La_{1.65}Nd_{0.35}CuO_4$. The arrows indicate the direction in which the magnetic field was changed during the experiment.

free charges in the CuO_2 plane as confirmed by a microprobe analysis which revealed an overall nonstoichiometric composition described by the chemical formula $La_{1.69}Nd_{0.336}Cu_{0.954}O_4$ (equivalent to $\delta \approx 0.007$ in $La_2CuO_{4+\delta}$). Actually, many recent studies have reported that $La_2CuO_{4+\delta}$ exhibits phase separation for δ down to 0.003.[38]

The magnetization measurements in fields applied along the *c* axis show that sample 1 is a weak ferromagnet at low temperatures (Fig. 8). The temperature variation of the remanent magnetization indicates that the weak ferromagnetism induced by the antisymmetric Dzyaloshinskii-Moriya (DM) interaction between the Cu spins[39] persists at $H=0$ T up to a temperature of about 15 K, in good agreement with available data.[14] We note that a metamagnetic transition, revealed in fields from 0.03 to 0.3 T by magnetization measurements, indicates a finite ferromagnetic moment vanishing at 20–25 K. The temperature dependence of the ferromagnetic component follows roughly the Curie-Weiss law, which is indicative of the essential contribution of the Nd^{3+} sublattice, magnetically polarized by the Nd-Cu coupling. The lifting of the degeneracy of the Nd^{3+} Kramers doublets due to this coupling is illustrated by the ~ 3.2 cm^{-1} splitting of the 1932 cm^{-1} absorption band at 9 K, shown in the inset of Fig. 3(a). To obtain the paramagnetic susceptibility anisotropy of sample 1 in an applied field of 0.15 T, displayed in Fig. 9, we have corrected the experimental susceptibility (χ) data in the perpendicular orientation for the ferromagnetic contribution.

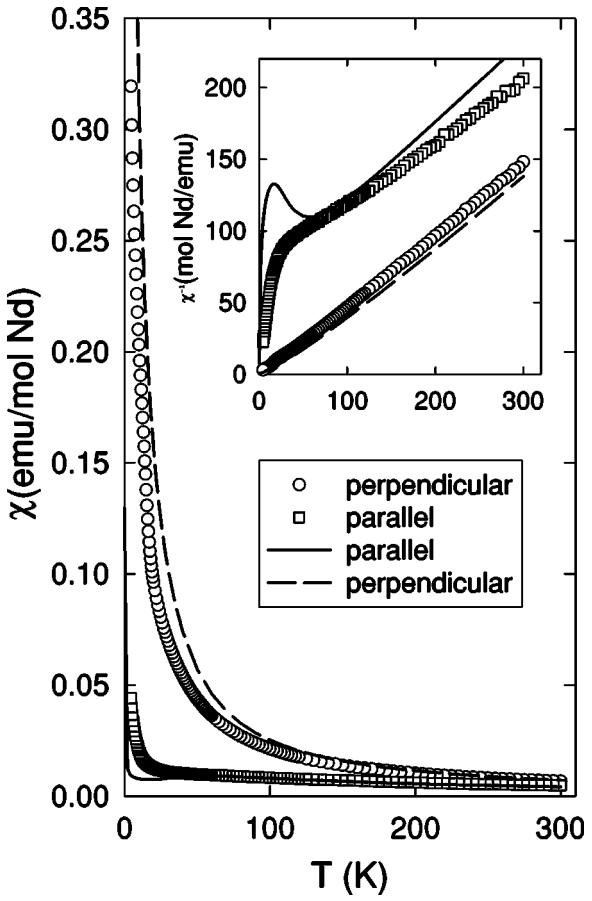

FIG. 9. Magnetic susceptibility measurements of $La_{1.65}Nd_{0.35}CuO_4$ (dots) and calculations (lines) parallel and perpendicular to the CuO_2 planes. Inset: inverse magnetic susceptibility.

In comparison to other Nd cuprates: Nd_2CuO_4 (Ref. 40) and $NdBa_2Cu_3O_6$,[41] the anisotropy, imprinted by the CF interaction at the Nd^{3+} sites, is much more pronounced and persists until room temperature. The theoretical χ vs T curve calculated using the best-fit CF parameters (Table I) is shown to compare well with the experimental data (Fig. 9). At 20 K, the susceptibility in parallel orientation is more than 20 times smaller than in the perpendicular orientation. The difference between these two directions further increases with decreasing temperature. We ascribe the nonobservation of the minimum in $\chi(T)$ [or the maximum in $\chi^{-1}(T)$] to an admixture of the perpendicular component into the parallel data due to the imperfect orientation of the applied magnetic field with respect to the crystal a-b plane. The calculated ground-state g-tensor values of Nd^{3+} in sample 1: $g_a = 0.373$, $g_c = 5.796$ indicate a very large Ising-like (Ref. 42) anisotropy of the low-temperature magnetic moment, much stronger than in any known Nd^{3+}-compound. This remarkably strong anisotropy is related to the high value of the 2^{nd} rank CF parameter B_{20}: e.g., its respective theoretical and best-fit values of 1123 and 1518 cm^{-1} (Table I) are three to four times larger than the corresponding values of 412 cm^{-1} (Ref. 43) and 380 cm^{-1} (Ref. 12) in $NdBa_2Cu_3O_6$. The difference between the theoretical B_{20} values in these two compounds is connected with a difference in the occupation of the p_x, p_y, and p_z orbitals in the $5p$ and $6p$ valence states as well as of the d_{z^2}, $d_{x^2-y^2}$, d_{xy}, d_{xz}, and d_{yz} orbitals in the valence $5d$ states of Nd^{3+} ion. Significant contribution to B_{20} from charges within the atomic sphere is proportional to the quantities ΔN_p and ΔN_d which are functions of the orbital occupation numbers.[44] We have obtained ΔN_p equal to -0.021 and -0.009 electrons and ΔN_d equal to -0.097 and -0.021 electrons for the Nd^{3+} ion in sample 1 and $NdBa_2Cu_3O_6$ compounds, respectively. Therefore, the extraordinary anisotropy of the Nd^{3+} magnetic moment in sample 1 is directly related to the anisotropy of the Nd-p and Nd-$5d$ occupied states in the close proximity of the maximum of the radial charge density distribution of the localized Nd-$4f$ states.

IV. CONCLUSIONS

We have reported on an Nd^{3+} CF infrared absorption study in $La_{2-x-y}Nd_xSr_yCuO_4$. 16 CF levels of the four first excited multiplets have been observed. The determination of the CF parameters for the C_{4v} symmetry site, using both *ab initio* and SM calculations, indicates a good agreement between the observed and calculated CF levels. A comparison between the theoretical model (calculated for the ideal La_2CuO_4 $I4/mmm$ structure) and the fit shows a fairly good agreement, excepted for the B_{40} CF parameter which is very sensitive to the apical oxygen position. As previously reported,[14] the magnetic susceptibility measurements display a weak ferromagnetic component below 15 K induced by an antisymmetric DM interaction. The measured paramagnetic susceptibility, which anisotropy is more pronounced than in any other Nd compound, compares well with the predictions of the CF parameters. Many additional absorption bands are associated with the presence of at least one nonregular Nd^{3+} site due to possible charge fluctuations and stripes.

ACKNOWLEDGMENTS

We thank J. Rousseau and M. Castonguay for technical assistance and P. Richard for fitting the data. G.R., S.J., and M.P acknowledge support from the National Science and Engineering Research Council of Canada (NSERC) and from le Fonds de Formation de Chercheurs et l'aide à la Recherche du Gouvernement du Québec. Also gratefully acknowledged are the Grant Agency of the Czech Republic for its Grants No. 202/00/1602 (V.N., M.M., and M.D.) and 203/02/0436 (J.F.) and the Grant Agency of Charles University for its Grant No. 145/2000/B-FYZ (M.D.). The work in Prague was also supported by institutional projects AV0Z1-010-914 and MSM113200002. Single crystal growth by means of the TSFZ method have been supported by the FOM-ALMOS. The work in Minsk was supported in part by NATO linkage Grant No. PST.CLG. 977766 and by INTAS in frame of Grant Nos. 96-0410 and 01-0278.

*Electronic address: griou@physique.usherb.ca
†Also at Institut Teknologi Bandung, Jl. Ganesha 10, Bandung 40132, Indonesia.

[1] J. M. Tranquada, B. J. Sternlieb, J. D. Axe, Y. Nakamura, and S. Uchida, Nature (London) **375**, 561 (1995).
[2] S. H. Lee, S. W. Cheong, K. Yamada, and C. F. Majkrzak, Phys. Rev. B **63**, 060405(R) (2001).
[3] Yu. G. Pashkevich, V. A. Blinkin, V. P. Gnezdilov, V. V. Tsapenko, V. V. Eremenko, P. Lemmens, M. Fischer, M. Grove, G. Güntherodt, L. Degiorgi, P. Wachter, J. M. Tranquada, and D. J. Buttrey, Phys. Rev. Lett. **84**, 3919 (2000).
[4] V. J. Emery, S. A. Kivelson, and O. Zachar, Phys. Rev. B **56**, 6120 (1997).
[5] S. H. Pan, E. W. Hudson, K. M. Lang, H. Eisaki, S. Uchida, and J. C. Davis, Science **403**, 746 (2000).
[6] C. Howald, P. Fournier, and A. Kapitulnik, Phys. Rev. B **64**, 100504 (2001).
[7] U. Staub and L. Soderholm, in *Handbook on the Physics and Chemistry of Rare Earths*, edited by K. A. Schneidner, Jr., L. Eyring, and M. B. Maple (Elsevier, Amsterdam, 2000), Vol. 30, p. 491.
[8] G. Riou, S. Jandl, M. Poirier, V. Nekvasil, M. Diviš, P. Fournier, R. L. Greene, D. I. Zhigunov, and S. N. Barilo, Eur. Phys. J. B **23**, 179 (2001).
[9] S. Jandl, T. Strach, T. Ruf, M. Cardona, V. Nekvasil, D. I. Zhigunov, S. N. Barilo, and S. V. Shiryaev, Physica C **322**, 87 (1999).
[10] S. Jandl, P. Richard, M. Poirier, V. Nekvasil, A. A. Nugroho, A. A. Menovsky, D. I. Zhigunov, S. N. Barilo, and S. V. Shiryaev, Phys. Rev. B **61**, 12 882 (2000).
[11] S. Jandl, T. Strach, T. Ruf, M. Cardona, V. Nekvasil, M. Iliev, D. I. Zhigunov, S. N. Barilo, and S. V. Shiryaev, Phys. Rev. B **56**, 5049 (1997).
[12] A. A. Martin, T. Ruf, M. Cardona, S. Jandl, D. Barba, V. Nekvasil, M. Diviš, and T. Wolf, Phys. Rev. B **59**, 6528 (1999).
[13] D. Barba, S. Jandl, V. Nekvasil, M. Maryško, M. Diviš, A. A. Martin, C. T. Lin, M. Cardona, and T. Wolf, Phys. Rev. B **63**, 054528 (2001).
[14] M. K. Crawford, R. L. Harlow, E. M. McCarron, W. E. Farneth, N. Herron, H. Chou, and D. E. Cox, Phys. Rev. B **47**, 11 623 (1993).
[15] J. D. Axe, A. H. Moudden, D. Hohlwein, D. E. Cox, K. M. Mohanty, A. R. Moodenbaugh, and Youwen Xu, Phys. Rev. Lett. **62**, 2751 (1989).
[16] M. K. Crawford, R. L. Harlow, E. M. McCarron, W. E. Farneth, J. D. Axe, H. Chou, and Q. Huang, Phys. Rev. B **44**, 7749 (1991).
[17] B. Nachumi, N. Ichikawa, Y. Nakamura, and S. Uchida, Phys. Rev. B **63**, 092103 (2001).
[18] J. M. Tranquada, N. Ichikawa, and S. Uchida, Phys. Rev. B **59**, 14712 (1999).
[19] J. M. Tranquada, J. D. Axe, N. Ichikawa, Y. Nakamura, S. Uchida, and B. Nachumi, Phys. Rev. B **54**, 7489 (1996).
[20] D. Lampakis, D. Palles, E. Liarokapis, C. Panagopoulos, J. R. Cooper, H. Ehrenberg, and T. Hartmann, Phys. Rev. B **62**, 8811 (2000).
[21] T. Kimura, K. Kishio, T. Kobayashi, Y. Nakayama, N. Motohira, K. Kitazawa, and K. Yamafuji, Physica C **192**, 247 (1992).
[22] S. N. Barilo, A. R. Ges, S. A. Guretskii, A. N. Luginets, A. I. Igumentsev, and V. N. Shambalev, J. Adv. Cryog. Eng. A **36**, 627 (1989).
[23] B. Nachumi, Y. Fudamoto, A. Keren, K. M. Kojima, M. Larkin, G. M. Luke, J. Merrin, O. Tchernyshyov, Y. J. Uemura, N. Ichikawa, M. Goto, H. Takagi, S. Uchida, M. K. Crawford, E. M. McCarron, D. E. MacLaughlin, and R. H. Heffner, Phys. Rev. B **58**, 8760 (1998).
[24] L. I. Buranov and I. F. Schegolev, Prib. Tekh. Eksp. **2**, 171 (1971).
[25] S. Jandl, P. Richard, J. Trottier, K. Frikach, M. Poirier, D. I. Zhigunov, S. N. Barilo, and S. V. Shiryaev, Physica C **297**, 64 (1998).
[26] K. Tamasaku, Y. Nakamura, and S. Uchida, Phys. Rev. Lett. **69**, 1455 (1992).
[27] W. E. Pickett, Rev. Mod. Phys. **61**, 433 (1989).
[28] A. W. Mombru, A. Lappas, and K. Prassides, J. Solid State Chem. **140**, 345 (1998).
[29] C. Görller-Walrand and K. Binnemans, in *Handbook on the Physics and Chemistry of Rare Earths*, edited by K. A. Gschneidner, Jr. and L. Eyring (Elsevier, Amsterdam, 1996), Vol. 23, p. 168.
[30] M. Roepke, E. Holland-Moritz, B. Büchner, H. Berg, R. E. Lechner, S. Longeville, J. Fitter, R. Kahn, G. Coddens, and M. Ferrand, Phys. Rev. B **60**, 9793 (1999).
[31] E. S. Bozin, G. H. Kwei, H. Takagi, and S. J. L. Billinge, Phys. Rev. Lett. **84**, 5856 (2000).
[32] M. Guttman, S. J. L. Billinge, E. Brosha, and G. H. Kwei, Physica C **341-348**, 2143 (2000).
[33] S. J. L. Billinge and T. Egami, Phys. Rev. B **47**, 14 386 (1993).
[34] A. Mirmelstein, A. Podlesnyak, V. Bobrovskii, and I. Zhdakhin, J. Phys.: Condens. Matter **11**, 7155 (1999).
[35] J. Mesot and A. Furrer, J. Supercond. **10**, 623 (1997); D. Rubio, J. Mesot, K. Conder, S. Janssen, H. Mutka, and A. Furrer, *ibid.* **13**, 727 (2000).
[36] V. Nekvasil, S. Jandl, T. Strach, T. Ruf, and M. Cardona, J. Magn. Magn. Mater. **177-181**, 535 (1998).
[37] N. L. Saini, H. Oyanagi, A. Lanzara, D. Di Castro, S. Agrestini, A. Bianconi, F. Nakamura, and T. Fujita, Phys. Rev. B **64**, 132510 (2001).
[38] X. L. Dong, Z. F. Dong, Z. X. Zhao, X. F. Duan, L.-M. Peng, W. W. Huang, B. Xu, Y. Z. Zhang, S. Q. Guo, L. H. Zhao, and L. Li, Phys. Rev. Lett. **80**, 2701 (1998); C. Chen, F. R. Wondre, and J. Ryan, Int. J. Mod. Phys. B **14**, 3406 (2000); Y. S. Lee, R. J. Birgeneau, M. A. Kastner, Y. Endoh, S. Wakimoto, K. Yamada, R. W. Erwin, S. H. Lee, and G. Shirane, Phys. Rev. B **60**, 3643 (1999).
[39] I. Dzyialoshinskii, J. Phys. Chem. Solids **4**, 241 (1958); T. Moriya, Phys. Rev. **120**, 91 (1960).
[40] Y. U. Muzichka, E. A. Goremychkin, I. V. Sashin, M. Diviš, V. Nekvasil, M. Nevriva, and G. Fillion, Solid State Commun. **82**, 461 (1992).
[41] V. Nekvasil, S. Jandl, D. Barba, A. A. Martin, M. Cardona, M. Diviš, M. Maryško, and T. Wolf, J. Magn. Magn. Mater. **226-230**, 985 (2001).
[42] W. P. Wolf, Braz. J. Phys. **30**, 794 (2000); V. Nekvasil, M. Diviš, G. Hilscher, and E. Holland-Moritz, J. Alloys Compd. **225**, 578 (1995).
[43] V. Nekvasil, S. Jandl, M. Cardona, M. Diviš, and A. A. Nugroho, J. Alloys Compd. **323-324**, 549 (2001).
[44] R. Coehorn and K. H. J. Buschow, J. Appl. Phys. **69**, 5590 (1991).